PCCP

Accepted Manuscript

ROYAL SOCIETY OF CHEMISTRY

www.rsc.org/pccp

PCCP

RSCPublishing

ARTICLE

On the photostability of peptides after selective photoexcitation of the backbone: Prompt *versus* slow dissociation

Cite this: DOI: 10.1039/xoxxoooooox

Received ooth January 2012,
Accepted ooth January 2012

DOI: 10.1039/xoxxoooooox

www.rsc.org/

Camilla Skinnerup Byskov, [a] Frank Jensen,[b] Thomas J.D. Jørgensen[c] and Steen Brøndsted Nielsen[a*]

Vulnerability of biomolecules to ultraviolet radiation is intimately linked to deexcitation pathways: Photostability requires fast internal conversion to the electronic ground state, but also intramolecular vibrational redistribution and cooling on a time scale faster than dissociation. Here we present a protocol to disentangle slow and non-hazardous statistical dissociation from prompt cleavage of peptide bonds by 210-nm light based on experiments on protonated peptides isolated *in vacuo* and tagged by 18-crown-6 ether (CE). The weakest link in the system is between the charged site and CE, which is remote from the initial site of excitation. Hence loss of CE serves as direct proof that energy has reached the charge-site end, leaving the backbone intact. Our work demonstrates that excitation of tertiary amide moieties (proline linkages) results in both prompt dissociation and statistical dissociation after energy randomisation over all vibrational degrees of freedom.

Introduction

Life on Earth arose about 3.5 billion years ago, prior to the presence of a protecting ozone layer, and high photostability of the "molecules of life" in the primordial soup against the intense solar irradiation in the ultraviolet region is likely to have been a crucial prerequisite. An electronically excited molecule is highly reactive and can undergo hazardous chemical reactions with other molecules or even unimolecular dissociation, and photostability is therefore governed by the efficiency of conversion from electronic energy into heat. Hence it is no surprise that the intrinsic photostability of biomolecules such as nucleic acids and peptides has become a field of intense research, both among spectroscopists and quantum chemists and physicists.[1-6] Also in sun screen and in photodynamic therapy, photostability is an issue. Important questions addressed are how quickly the photoexcited chromophore returns to its electronic ground state, the involved potential energy surfaces and the occurrence of ultrafast radiationless transitions where two surfaces touch each other (conical intersection), the time scale for intramolecular vibrational redistribution (IVR) of the energy, and finally how fast the excitation energy dissipates to a nearby environment, *e.g.* water molecules.

A wealth of information has been obtained from gas-phase spectroscopy experiments and excited-state calculations on isolated molecules and ions as there the fate of the photoactive part is most easily deduced and its intrinsic properties revealed.[3,4,6-10.] Excitation of either a single localised chromophore or of one that appears throughout the molecule is performed. In the case of peptides, the former method includes excitation of the side-chains of aromatic amino acid residues using 260-270 nm ultraviolet light[8-11] and the latter excitation of backbone peptide linkages using more energetic photons[12-15]. Previous work by Jouvet and co-workers[8] on protonated aromatic amino acids showed that photo-induced dissociation (PID) to a large extent is governed by the coupling between the excited state located on the chromophore and the dark (*i.e.*, low oscillator strength) $\pi\sigma^*$ state on the ammonium group. Charge transfer results in a hypervalent nitrogen and subsequent dissociation by loss of hydrogen or ammonia. This non-statistical pathway was seen for excitation of the peptide chromophores as well but could be eliminated by moving the ammonium $\pi\sigma^*$ state out of the spectral region by *e.g.* crown-ether attachment as demonstrated by Brøndsted

Nielsen and co-workers[11] or microhydration (work by Rizzo and co-workers[16]). Competing deactivation processes involving charge transfer to carbonyl groups and coupled proton movement, followed by prompt dissociation were also identified. In a recent work by Mons, Ljubić and co-workers[17] and highlighted by Domcke and Sobolowski[18], the importance of peptide folding for deactivation via an electron-driven proton transfer mechanism along hydrogen bonds was demonstrated.

There are several reports on the dissociation of protonated peptides after photoexcitation of amide chromophores by either 157-nm or 193-nm light;[12-15] these wavelengths are easily produced by an ArF excimer laser and an F_2 laser, respectively. One motivation for these experiments was to develop an efficient method for the fragmentation of large peptides and proteins. Indeed, at these wavelengths, energy is imparted into the backbone with the possibility of informative sequence fragments without energy redistribution. Photon energies are 6.4 eV and 7.9 eV, which is more than sufficient to cleave peptide bonds requiring 3-4 eV. In particular, the occurrence of site-directed cleavages would be valuable not only for sequencing but also to pinpoint posttranslational modifications.[15] First pioneering work was done by McIver's group[12] in the eighties and work has continued up to today by the groups of D.F. Hunt, D.H. Russell, K. Biemann, F.W. McLafferty, M.S. Kim, R.A. Zubarev, J.S. Brodbelt, P. Dugourd, R.R. Julian, and J.P. Reilly (discussed in recent reviews)[13-15]. The current status is that PID of singly or multiply protonated peptides is quite efficient and dominated by scission of C_α-C(O) and C(O)–N bonds to give a series of *a*, *x* and *b*, *y* fragments (nomenclature is defined in Fig. 1, *vide infra*), but side-chain cleavages are also seen. *b* and *y* ions dominate low-energy collision-induced dissociation (CID) that is inherently statistical, and one explanation for their formation in PID could be internal conversion (IC) followed by IVR. In this case all memory of the initial excited state is lost and dissociation is governed by the mobile proton model[19] where the excess energy allows the protons to move to the amide groups and thereby lowering the C(O)–N bond energies. Little is still known about the energy-conversion processes after photo-excitation of the backbone, and it remains to be proven that dissociation of the peptide bond occurs directly from the excited state or before IVR on the ground-state potential energy surface. Such dissociation is termed non-statistical while dissociation following statistical equilibration of the excess energy over all degrees of freedom is termed statistical.

To our knowledge, selective excitation of specific amide groups has not been studied, and it is unknown if dissociation would dominantly occur at these groups. The problem is to disentangle dissociation due to statistical dissociation from that due to prompt dissociation, which is particularly difficult when the dissociation channels are very similar! Prompt dissociation here implies dissociation prior to randomisation of the excess energy over all degrees of freedom, *i.e.*, it is non-statistical. In the present work we provide a solution to the above problem based on a simple approach where protonated proline-containing peptides tagged with 18-crown-6 ether (CE) are photodissociated with 210-nm light. A preferred site of CE binding is the protonated ε-amino side-chain of lysine.[20] The interpretation of the results is aided by quantum-chemical calculations of geometrical structures, dissociation energies, and excited states. Model peptides chosen for the study are PPK, KPP, PPPK, RPPK, KP, KW, WK, and RW (P = proline, K = lysine, R = arginine, W = tryptophan). Our results allow us to quantify the branching between statistical and non-statistical dissociation after excitation of amide groups. The reason for the choice of proline is discussed in the following along with the idea behind crown-ether tagging.

Earlier work by Kuipers and Gruppen[21] showed that when proline participates in a peptide bond (tertiary amide), the extinction coefficient is significantly higher, by a factor of three at 214 nm compared to other peptide linkages. This finding was based on solution-phase spectroscopy of triglycine and tripeptides with two glycines and one proline, in which proline is present at the N terminus, C terminus, and in the middle of the chain. The larger extinction coefficient implies that the energy is deposited at proline peptide linkages with a higher probability than at other sites, which potentially could lead to a certain degree of selectivity in the excitation. The work indicated that neighbour prolines further strengthen absorbance but more work is needed to confirm this.

We therefore chose proline-containing peptides for the present work to selectively excite the tertiary amide group. Another important advantage of proline linkages is that the available conformational phase space is smaller than for non-cyclic ones and thus reducing the number of important structures in the ion beam. A possible complication in the analysis is that dissociation of proline linkages after photoexcitation of the protonated peptides *in vacuo* could be favoured simply because of the higher proton affinity of a tertiary amide compared to a secondary one, which is relevant as according to the mobile proton model the amides compete for the excess proton, rather than being the results of prompt dissociation following selective excitation. To firmly establish the occurrence of non-statistical prompt dissociation, it is therefore necessary to immobilise excess protons that govern statistical fragmentation of "hot" peptide cations, which is done by tagging ammonium groups by CE thereby keeping the protons sequestered at the nitrogen. Even though CE is optimal for binding to $–NH_3^+$, it requires less energy to lose it (about 2 eV)[22] than to break the backbone (*vide infra*). Loss of CE is therefore direct evidence for statistical dissociation while breakage of the peptide backbone without dissociating CE is evidence of non-statistical dissociation. Finally, to exclude the possibility of backbone dissociation as a competitive statistical dissociation process, we carried out low-energy and high-energy collision experiments in which fragment ions from vibrationally excited peptides were measured.

Experimental

Synthetic peptides were purchased from LifeTein LLC (Hillsborough, NJ, USA) and 18-crown-6 ether from Sigma-Aldrich. Peptides were dissolved in a water/methanol solution (1:1) with 10 % acetic acid added. CE was added to the solutions to produce complexes with one CE attached.

Two instrumental setups were used for photodissociation experiments and low-energy collisions, respectively, described separately in the following. PID was done with a home-built mass spectrometer combined with a pulsed, tuneable laser system.[23] The latter is a 20-Hz Nd:YAG with the 1064-nm fundamental frequency tripled to 355 nm. This UV light is split into 420-nm blue light and 2300-nm infrared light in an optical parametric oscillator (OPO) followed by a frequency doubling of the visible light in a barium borate (BBO) crystal to produce 210-nm light. The ions were produced in an electrospray ionisation source, trapped in an octopole ion trap and extracted every 25 ms. Following extraction, the ions were accelerated through 50 kV, and ions of interest were selected with a bending magnet according to their mass-to-charge ratio (*m/z*). An interaction region of 1.8 m follows the magnet, in which photoexcitation of the ion bunch was done. In order to obtain both a laser-on and a laser-off signal, only every second ion bunch was irradiated with the laser light. The laser-off signal arises from

collisions between ions and residual gas in the beam line (the pressure was around 10^{-6} mbar) and from metastable decay of vibrationally excited ions. Fragment ions were analysed in a hemispherical, electrostatic analyser and counted with a channeltron detector. PID spectra were obtained by subtracting the laser-off signal from the laser-on signal.

Low-energy CID experiments were carried out using a Synapt G2 HDMS quadrupole-time-of-flight mass spectrometer (Waters Corporation, Milford, MA, USA). Product ions were generated by collisions with argon gas in the T-wave trap collision cell (gas pressure 7.6×10^{-3} mbar). Peptide solutions were infused into the electrospray ion source at a flow rate of 10 μL/min. The source settings were as follows: ion source temperature 100°C; dinitrogen was used as desolvation gas (flow rate 800 L/h, temperature 250°C); capillary voltage 3.0 kV; sampling cone voltage 30 V.

Calculations

The conformational spaces of $[PPK+H]^+$ and $[PPK+H]^+$(CE) were searched using the OPLS2005 force field as implemented in the Macromodel module in Maestro 9.5 (Schrödinger, Inc.).[24,25] All 606 conformers within 30 kJ/mol of the lowest-energy structure were analysed by non-hydrogen atomic root mean squared deviations RMSD into 20 clusters. Density Functional Theory (DFT) using the wB97xd functional[26], and the pcseg-1 basis set[27] was used to optimise the lowest-energy structure from each cluster using the Gaussian-09 program.[28] Time-Dependent (TD) - DFT calculations were done using the same functional and the aug-pcseg-1 basis set.

Results and discussion

The PID mass spectrum of $[PPK+H]^+$ obtained after 210-nm photoexcitation is shown in Fig. 1a. It is evident that dominant fragment ions are a_1^+, y_2^+, a_2^+, and y_1^+. The former two are due to cleavages at the N-terminal amide site while the latter two arise from cleavages at the C-terminal amide site. The a_1^+ and y_2^+ ions are most abundant in accordance with both statistical and non-statistical dissociation processes. Loss of ammonia from the y_2^+ ion is also seen. The peak at *m/z* 84 corresponds to a common fragment of lysine-containing peptides.[29,30] The spectrum contains a few other peaks that have not been assigned. As mentioned above, this spectrum does not by itself shed light on the deexcitation pathway(s).

Fig. 1b shows the PID spectrum of the crown-ether complex, $[PPK+H]^+$(CE). The number of fragment ions is significantly reduced compared to the bare peptide. The most likely process is simply loss of CE to give $[PPK+H]^+$. There is also a peak corresponding to formation of y_2^+(CE) with an abundance of 34 % of the $[PPK+H]^+$ ion. CE preferably binds to the ε-ammonium group of lysine, and y_2^+(CE) is therefore direct evidence for rupture of the N-terminal C(O)–N bond. Minor peaks correspond to y_2^+ and a_1^+ that could be formed from $[PPK+H]^+$ daughter ions in a consecutive process, or y_2^+ could be formed from y_2^+(CE). This experiment unambiguously shows that statistical fragmentation (CE loss) is the dominant process after photoexcitation of amide groups. It does, however, leave room for some prompt fragmentation to account for the y_2^+(CE) ion. To confirm that this ion is not due to statistical fragmentation in competition with CE loss, we carried out both low-energy and high-energy collision experiments (Fig. 1c,d). In the low-energy experiment, the ions dissociated after multiple collisions with argon gas in a collision cell. The initial collision energy was 30 eV in the laboratory frame, which corresponds to 1.9 eV in the center-of-mass frame. The spectrum is quite simple: The dominant fragment ion is due to loss of CE. A minor peak corresponds to y_2^+ that is most likely due to further dissociation of $[PPK+H]^+$. At 60-eV collision energies (laboratory frame), more lower mass fragment ions appear (supporting information), but there is no indication of the formation of y_2^+(CE). The high-energy collision spectrum that was recorded under single-collision conditions and 50-keV collision energies is surprisingly similar to the low-energy one except for the clear presence of a_1^+ ions. In this experiment, dissociation can be both due to electronic and nuclear (vibrational excitation) stopping processes[31]. The range of internal energies is much higher than that in the low-energy experiment, but again we conclude that y_2^+(CE) ions are not formed to any significant degree.

For comparison, experiments were also done on KPP that contains two tertiary amide linkages. Indeed, photoexcitation of $[KPP+H]^+$(CE) leads to both a_1^+(CE) and a_2^+(CE) ions in almost equal abundances (Fig. 1e). These ions were not formed after collisional excitation (*cf.*, supporting information). Minor yield of b_1^+(CE) is also observed. The total abundance of these three ions relative to $[KPP+H]^+$ is about 36 %, and the dominant process is therefore still loss of CE, confirming the rapid deexcitation and energy randomisation after photoexcitation of amide groups.

Taken together, the formation of y_2^+(CE) from $[PPK+H]^+$(CE) and a_1^+(CE) and a_2^+(CE) from $[KPP+H]^+$(CE) is specific to 210-nm photoexcitation and is an indication of prompt dissociation processes, either directly on an excited-state surface or after IC but prior to IVR. Interestingly, the absence of y_1^+(CE) (PPK) is in accordance with a higher oscillator strength of the tertiary amide relative to that of the secondary amide, and while this by itself does not prove prompt fragmentation, it certainly is in support.

Based on molecular dynamics calculations on $[PPK+H]^+$(CE) we identified 606 structures. These were divided in 20 clusters and the one from each cluster with lowest energy was re-optimised with DFT. Their relative energies are all within 30 kJ/mol, and these could all be present under our experimental conditions (room temperature). The crown ether binds to the charge site and other configurations are too high in energy to be of relevance. A representative geometry is shown in Fig. 2 together with natural transition orbitals[32] of the lowest TD-DFT excited state. DFT calculations reveal that CE loss requires about 2 eV[22] while breakage of the backbone to give y_2^+(CE) and b_1 is more costly, typically 2.7-5.1 eV (range determined by the different structural motifs) in good agreement with our experimental observations. Fig. 2 also shows the energies of the first three excited states relative to the ground state, obtained from TD-DFT, for all the geometrical structures. The S_1 state is more likely located on the tertiary amide than on the secondary one while the opposite is the case for S_2. The oscillator strength is slightly larger for S_2 than for S_1. However, as we in our experiment excite at the red end of the absorption bands, it is more probable to excite S_1(tertiary amide) than S_2(secondary amide) but even in the latter case quick IC from S_2 to S_1 would lead to more excited tertiary amides than secondary ones. The S_3 state is mainly located on the carboxylic acid group and is of smaller importance though again quick IC via S_2 would lead to S_1. Overall the theoretical calculations suggest cleavage on the S_1 potential-energy surface to account for the experimental observations.

In the following we corroborate our conclusions from the experimental results on the other peptides. The PPPK peptide contains one more proline linkage than PPK but the same number as KPP. The obtained spectra are shown in Fig. 3. Again y^+ and a^+ are the most abundant daughter ions after photoexcitation of the bare protonated peptide while the dominant dissociation process of the crown-ether complex is loss of CE. However, the formation of y_2^+(CE) and y_3^+(CE) ions is clearly seen and to a smaller extent

y_1^+(CE). Their abundance relative to $[PPPK+H]^+$ is 24 %. Both low-energy and high-energy collision experiments showed no evidence for the formation of these ions from vibrationally excited ions. Hence we conclude that these ions are formed in non-statistical processes. It should be noticed that the dominant fragmentation again occurs at tertiary amide linkages which are the sites where the initial energy is deposited with highest probability.

The next peptide was RPPK that has two basic residues; the guanidine group of the arginine side-chain and the ε-amino group of lysine. As a result the ion beam is likely composed of several different protonated forms. Indeed, the PID mass spectrum of the bare peptide contains *a*, *b*, and *y* ions (Fig. 4). Photoexcitation of $[RPPK+H]^+$(CE) reveals CE loss as the dominant observable process but also the formation of a_1^+(CE), a_2^+(CE), and a_3^+(CE); the latter ion barely discernible. The ratio between the yields of these three ions and $[RPPK+H]^+$ is 19 %. The presence of *a* ions indicate that the protonation site (and therefore also where the CE is located) is the N-terminal arginine. With regard to collision-induced dissociation, the story repeats itself: CE loss dominates, and there is no sign of a_1^+(CE), a_2^+(CE), and a_3^+(CE). We assign the a^+(CE) ions formed after photoexcitation to be due to prompt fragmentation, and assume that this again occurs preferentially at tertiary amide linkages.

Finally, experiments were done for KW, WK, and RW that have no tertiary amide linkage. Here the chromophore is the indole group of tryptophan as this has more than an order of magnitude higher absorption cross section than secondary amide groups.[21] The photoinduced fragmentation chemistry of the bare protonated peptides is rich (supporting information), and likely fragmentation is governed not only by statistical fragmentation but also fragmentation following electron transfer from the indole group to the charge site, the amide group, or the carboxylic acid group as discussed in detail for protonated tryptophan[33]. We will not discuss these spectra further as more experiments would be needed to firmly establish the mechanisms. More importantly, the PID spectra of the CE complexes reveal CE loss to be by far the most dominant process (Fig. 5). Dissociations at the amide groups are minor, being less than 4 % of the loss of CE. Previously reported UV PID spectra of $[AY+H]^+$(CE) and $[YA+H]^+$(CE) (A = alanine and Y = tyrosine) where tyrosine is the strongest UV chromophore are in accordance with these results as here it was also concluded that the CE switched off the C(O)–NH bond cleavage.[11] For comparison, we have included in the figure the PID spectrum of $[KP+H]^+$(CE) where the tertiary amide is the site of excitation, and now the ratio between the abundance of a_1^+(CE) and $[KP+H]^+$ is 61 %, more than an order of magnitude higher than those for the W-containing dipeptides. These findings support our previous conclusions that breakage of peptide bonds requires the energy to be deposited here; in other words, providing the peptides with the same amount of energy in a different way does not suffice to cleave the backbone.

Table 1 summarises the total yield of backbone cleavages relative to crown-ether loss for each peptide under study. Each full-scan spectrum took more than an hour to record, and as we cannot correct for ion-beam fluctuations, the numbers in the table were obtained by selected-ion monitoring of the relevant fragment ions and averaging over at least three measurements. It is evident that the ratio decreases with the size of the peptide. One plausible explanation is that for larger peptides, the two fragments formed after prompt dissociation stay together as an ion-molecule complex with a lifetime longer than the time for sampling dissociation in the experiment (about 10 μs). In support of this, we find that the yield of fragment ions arises both from one-photon and two-photon absorption; the absorption of a second 5.9-eV photon would certainly bring the dissociation time within the experimental time window. It should also be mentioned that after rupture of the N-C_α bond by electron attachment, the two fragments are sticking together long enough to allow for proton transfer and hydrogen atom transfer.[34-36] Another issue to consider is differences in folding motifs, and the possibility that only certain conformations are prone to prompt dissociation. More work is clearly needed to fully explain these differences in branching ratios.

Conclusions

We have shown that the initial site of photoexcitation of a peptide determines its dissociation channels, which indicates that non-statistical (prompt) dissociation plays a role. In a statistical dissociation process, the time scale for randomisation of the excess energy over all degrees of freedom is shorter than that of dissociation, and the origin of the energy is unimportant. Importantly, to photodissociate the backbone of a protonated peptide for which the protons are immobilised by crown-ether tagging, it is necessary to photoexcite the amide groups directly. When the photon is instead absorbed by an amino-acid residue with an aromatic chromophore, the backbone remains intact, and enough energy never accumulates in the amide group needed for its dissociation. In general, as soon as internal conversion and IVR have occurred, the possibility of backbone dissociation is fully lost since this channel cannot compete with crown-ether loss. Also our data are in agreement with higher oscillator strength at 210-nm excitation energy of tertiary amide linkages than that of secondary ones as dissociation mainly occurs at the former sites. Dissociation is not only governed by prompt cleavages but also slow statistical dissociation. This quick and efficient energy conversion and transport along the backbone provides photostability to the peptide after exposure to 210-nm irradiation. Future work aiming at describing in detail by theory the excited-state surfaces and how energy conversion occurs would be highly illuminating.

Acknowledgements

SBN gratefully acknowledges Lundbeckfonden for support and TJDJ the Carlsberg Foundation (grant no. 2012_01_0332). Eva C. Østerlund (SDU) is greatly acknowledged for technical assistance with mass spectrometry measurements.

Notes and references

[a] Department of Physics and Astronomy, Aarhus University, DK-8000 Aarhus C, Denmark. E-mail: sbn@phys.au.dk.

[b] Department of Chemistry, Aarhus University, DK-8000 Aarhus C, Denmark.

[c] Department of Biochemistry and Molecular Biology, University of Southern Denmark, DK-5230 Odense M, Denmark.

Electronic Supplementary Information (ESI) available: Low-energy CID, high-energy CID, and PID spectra of protonated peptides and complexes with crown ether. See DOI: 10.1039/b000000x/

1 C. E. Crespo-Hernandez, B. Cohen and P. M. Hare, *Chem. Rev.*, 2004, **104**, 1977.

2 D. Markovitsi, *Pure Appl. Chem.*, 2009, **81**, 1635.

3 K. Kleinermanns, D. Nachtigallova and M. S. de Vries, *Int. Rev. Phys. Chem.*, 2013, **32**, 308.
4 M. Perot, B. Lucas, M. Barat, J. A. Fayeton and C. Jouvet, *J. Phys. Chem. A*, 2010, **114**, 3147.
5 A. B. Stephansen, R. Y. Brogaard, T. S. Kuhlman, L. B. Klein, J. B. Christensen and T. I. Sølling, *J. Am. Chem. Soc*,. 2012, **134**, 20279.
6 R. Weinkauf, J. P. Schermann, M. S. de Vries and K. Kleinermanns, *Eur. Phys. J. D*, 2002, **20**, 309.
7 S. Brøndsted Nielsen, J. U. Andersen, J. S. Forster, P. Hvelplund, B. Liu, U. V. Pedersen and S. Tomita, *Phys. Rev. Lett*, 2003, **91**, 048302.
8 A. L. Sobolewski, W. Domcke, C. Dedoner-Lardeux and C. Jouvet, *Phys. Chem. Chem. Phys.*, 2002, **4**, 1093.
9 G. Aravind, B. Klærke, J. Rajput, Y. Toker, L. H. Andersen, A. V. Bochenkova, R. Antoine, J. Lemoine, A. Racaud and P. Dugourd, *J. Chem. Phys.*, 2012, **136**, 014307.
10 L. Joly, R. Antoine, M. Broyer, P. Dugourd and J. Lemoine, *J. Mass Spectrom.*, 2007, **42**, 818.
11 J. A. Wyer, A. Ehlerding, H. Zettergren, M.-B. S. Kirketerp and S. Brøndsted Nielsen, *J. Phys. Chem. A*, 2009, **113**, 9277.
12 W. D. Bowers, S.-S. Delbert, R. L. Hunter and R. T. McIver, Jr., *J. Am. Chem. Soc.*, 1984, **106**, 7288.
13 J. P. Reilly, *Mass Spectrom. Rev.*, 2008, **28**, 425.
14 T. Ly and R. R. Julian, *Angew. Chem. Int. Ed.*, 2009, **48**, 7130.
15 J. S. Brodbelt, *Chem. Soc. Rev.* 2014. DOI: 10.1039/c3cs60444f.
16 S. R. Mercier, O. Boyarkin, A. Kamariotis, M. Guglielmi, I. Tavernelli, M. Cascella, U. Rothlisberger and T. R. Rizzo, *J. Am. Chem. Soc.*, 2006, **128**, 16938.
17 M. Malis, Y. Loquais, E. Gloaguen, H. S. Biswal, F. Piuzzi, B. Tardivel, V. Brenner, M. Broquier, C. Jouvet, M. Mons, N. Doslic and I. Ljubic, *J. Am. Chem. Soc.*, 2012, **134**, 20340.
18 W. Domcke and A. L. Sobolewski, *Nature Chem.*, 2013, **5**, 257.
19 V. H. Wysocki, G. Tsaprailis, L. L. Smith and L. A. Breci, *J. Mass Spectrom.*, 2000, **35**, 1399.
20 R. R. Julian and J. L. Beauchamp, *Int. J. Mass Spectrom.*, 2001, **210**, 613.
21 B. J. H. Kuipers and H. Gruppen, *J. Agric. Food Chem.*, 2007, **55**, 5445.
22 A. I. S. Holm, M. K. Larsen, S. Panja, P. Hvelplund, S. Brøndsted Nielsen, R. D. Leib, W. A. Donald, E. R. Williams, C. Hao and F. Turecek, *Int. J. Mass Spectrom.*, 2008, **276**, 116.
23 K. Støchkel, B. F. Milne and S. Brøndsted Nielsen, *J. Phys. Chem. A*, 2011, **115**, 2155.
24 Maestro, version 9.5, Schrödinger, LLC, New York, NY, 2013.
25 MacroModel, version 9.8 (2010) Schrödinger, LLC, New York, NY.
26 J.-D. Chai and M. Head-Gordon, *Phys. Chem. Chem. Phys.*, 2008, **10**, 6615.
27 F. Jensen, *J. Chem. Theory Comput*, 2014, **10**, 1074.
28 Gaussian 09, Revision A.02, M. J. Frisch, G. W. Trucks, H. B. Schlegel, G. E. Scuseria, M. A. Robb, J. R. Cheeseman, G. Scalmani, V. Barone, B. Mennucci, G. A. Petersson, H. Nakatsuji, M. Caricato, X. Li, H. P. Hratchian, A. F. Izmaylov, J. Bloino, G. Zheng, J. L. Sonnenberg, M. Hada, M. Ehara, K. Toyota, R. Fukuda, J. Hasegawa, M. Ishida, T. Nakajima, Y. Honda, O. Kitao, H. Nakai, T. Vreven, J. A. Montgomery, Jr., J. E. Peralta, F. Ogliaro, M. Bearpark, J. J. Heyd, E. Brothers, K. N. Kudin, V. N. Staroverov, R. Kobayashi, J. Normand, K. Raghavachari, A. Rendell, J. C. Burant, S. S. Iyengar, J. Tomasi, M. Cossi, N. Rega, N. J. Millam, M. Klene, J. E. Knox, J. B. Cross, V. Bakken, C. Adamo, J. Jaramillo, R. Gomperts, R. E. Stratmann, O. Yazyev, A. J. Austin, R. Cammi, C. Pomelli, J. W. Ochterski, R. L. Martin, K. Morokuma, V. G. Zakrzewski, G. A. Voth, P. Salvador, J. J. Dannenberg, S. Dapprich, A. D. Daniels, Ö Farkas, J. B. Foresman, J. V. Ortiz, J. Cioslowski and D. J. Fox, Gaussian, Inc., Wallingford CT, 2009.
29 N. N. Dookeran, T. Yalcin and A. G. Harrison, *J. Mass Spectrom.*, 1996, **31**, 500.
30 W. Kulik and W. Heerma, *Biomed. Environ. Mass Spectrom.*, 1988, **15**, 419.
31 H. Zettergren, Personal Communication.
32 R. L. Martin, *J. Chem. Phys.*, 2003, **118**, 4775.
33 B. Lucas, M. Barat, J. A. Fayeton, M. Perot, C. Jouvet, G. Grégoire and S. Brøndsted Nielsen, *J. Chem. Phys.*, 2008, **128**, 164302.
34 C.S. Jensen, J. A. Wyer and S. Brøndsted Nielsen, *Phys. Chem. Chem. Phys.*, 2010, **12**, 12961.
35 P. B. O'Connor, C. Lin, J. J. Courmoyer, J. L. Pittman, M. Belyayev and B. A. Budnit, *J. Am. Soc. Mass Spectrom.*, 2006, **17**, 576.
36 F. Turecek and R. R. Julian, *Chem. Rev.*, 2013, **113**, 6691.

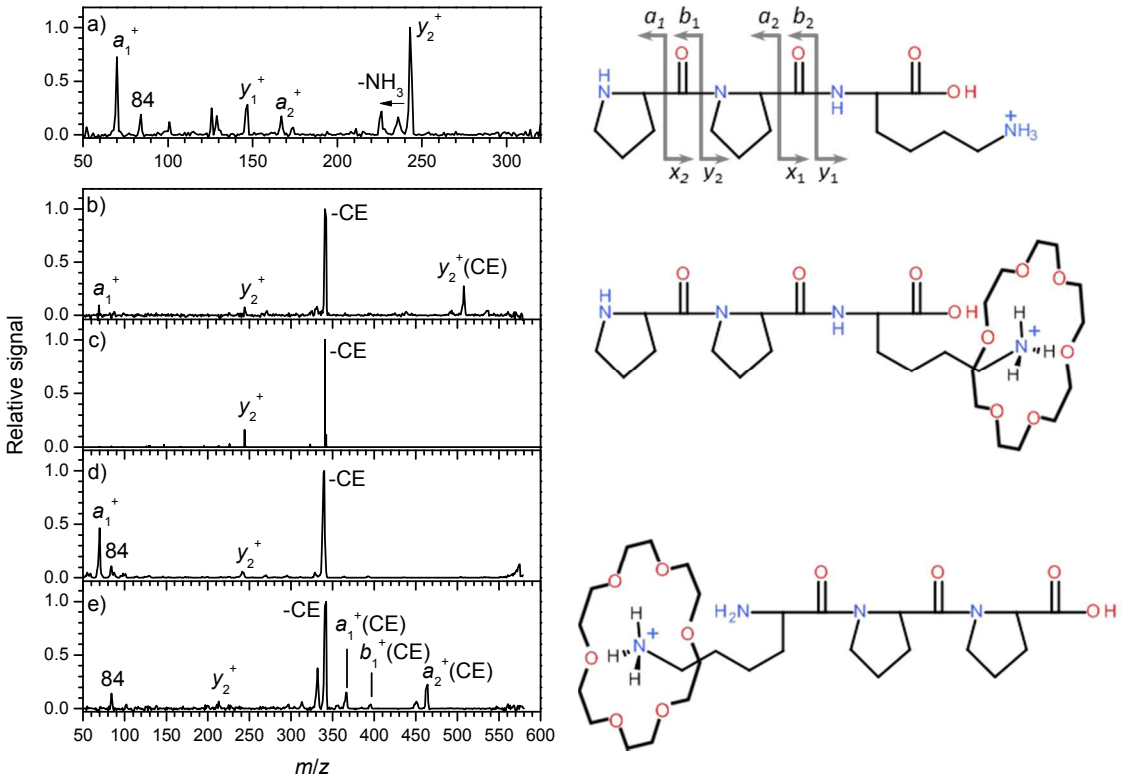

Fig. 1: PID mass spectra of (a) $[PPK+H]^+$ (*m/z* 341) and (b) $[PPK+H]^+(CE)$ (*m/z* 605), λ = 210 nm. (c) Low-energy CID mass spectrum of $[PPK+H]^+(CE)$, collision energy 30 eV in the laboratory frame. d) High-energy CID mass spectrum of $[PPK+H]^+(CE)$. e) PID mass spectrum of $[KPP+H]^+(CE)$ (*m/z* 605). Peptide structures are shown to the right.

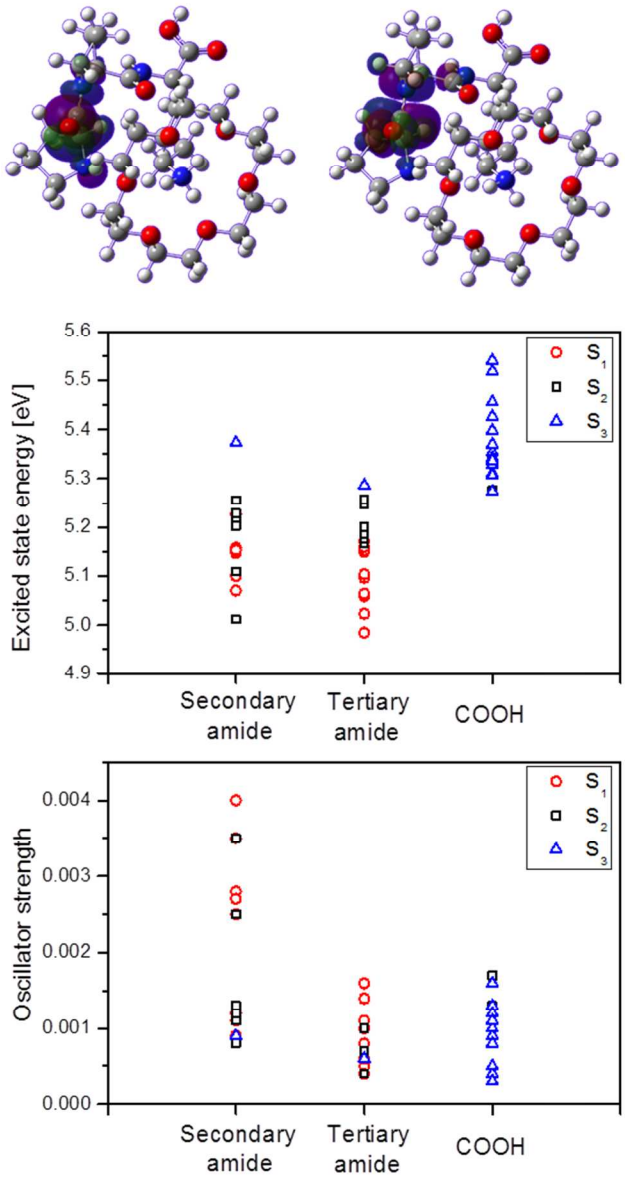

Fig. 2: Theoretical calculations. One representative low-energy structure of $[PPK+H]^+$(CE) is shown with the hole (left) and particle (right) natural transition orbitals for the S_0 to S_1 transition. The localised nature of the excitation of a tertiary amide is evident. Excited state energies and oscillator strengths for the three lowest states relative to the ground state are given for all the obtained low-energy structures and whether the excited state is located mainly on the secondary amide, the tertiary amide, or the carboxylic acid group.

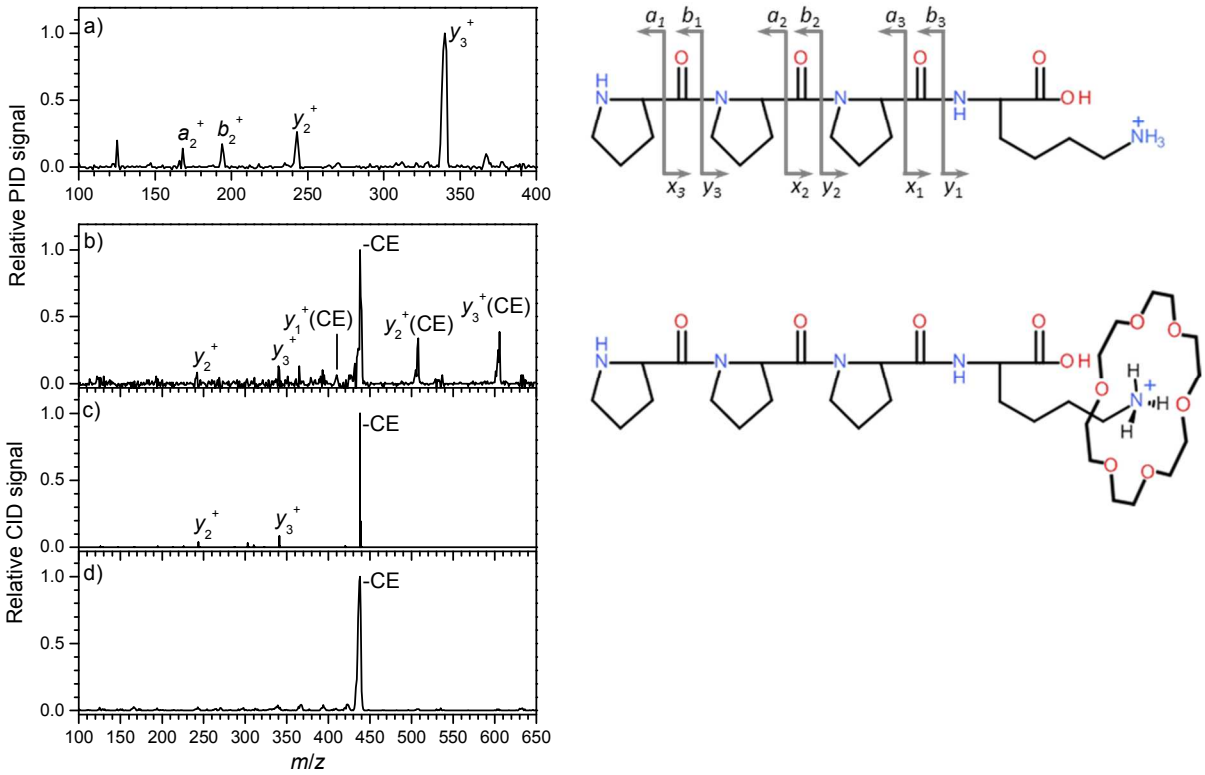

Fig: 3: PID mass spectra of (a) $[PPPK+H]^+$ (*m/z* 438) and (b) $[PPPK+H]^+(CE)$ (*m/z* 702), λ = 210 nm. (c) Low-energy CID mass spectrum of $[PPPK+H]^+(CE)$, collision energy 30 eV in the laboratory frame. (d) High-energy CID mass spectrum of $[PPPK+H]^+(CE)$. Peptide structures are shown to the right.

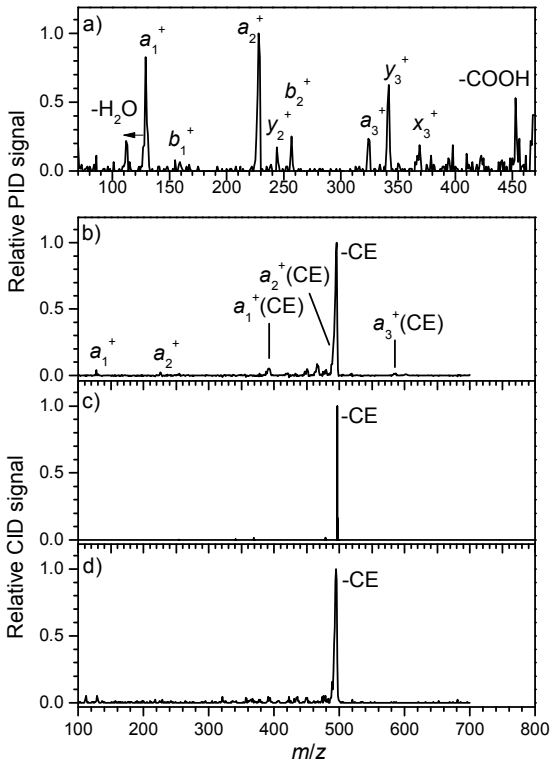

Fig. 4: PID mass spectra of (a) $[RPPK+H]^+$ (*m*/*z* 497) and (b) $[RPPK+H]^+(CE)$ (*m*/*z* 761), λ = 210 nm. (c) Low-energy CID mass spectrum of $[RPPK+H]^+(CE)$, collision energy 30 eV in the laboratory frame. (d) High-energy CID mass spectrum of $[RPPK+H]^+(CE)$.

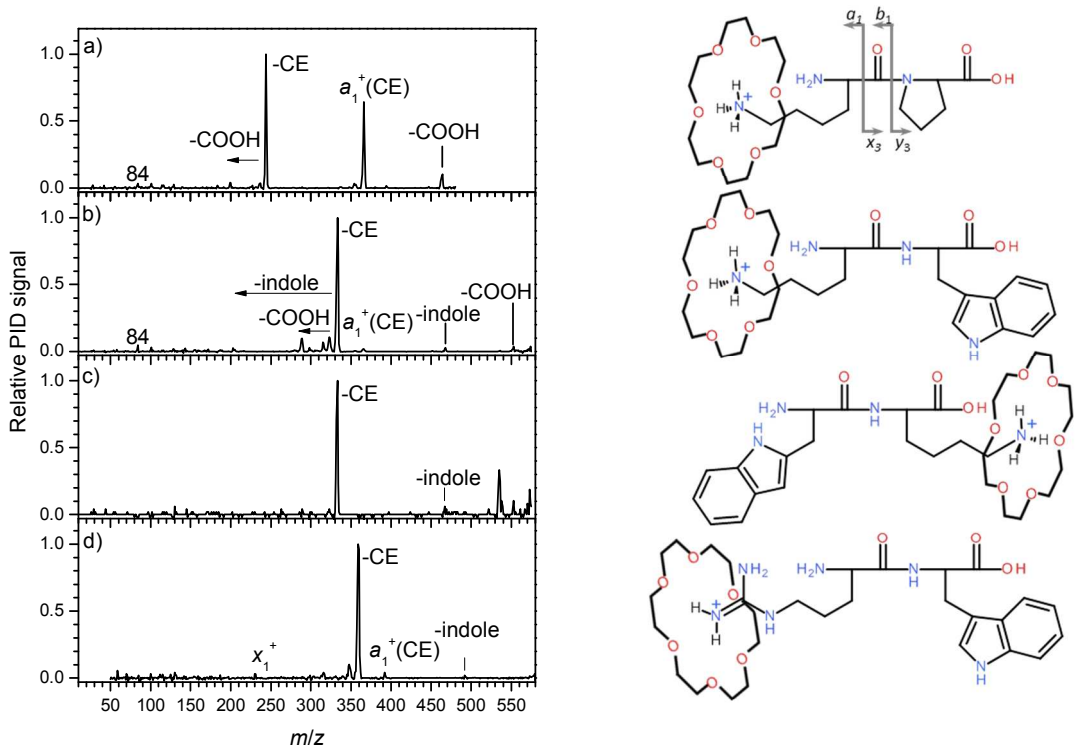

Fig. 5: PID mass spectra of (a) $[KP+H]^+$(CE) (*m/z* 508), (b) $[KW+H]^+$(CE) (*m/z* 597), (c) $[WK+H]^+$(CE) (*m/z* 597), and (d) $[RW+H]^+$(CE) (*m/z* 625), λ = 210 nm. Peptide structures are shown to the right.

Table 1. The ratio between total yield of prompt peptide-backbone cleavage and that due to loss of crown ether after 210-nm photoexcitation of protonated peptides tagged with crown ether.

Peptide	PPK	KPP	PPPK	RPPK	KP	KW	WK	RW
Chromophore	Amide					Indole		
Ratio	0.34	0.36	0.24	0.19	0.61	0.04	0.00	<0.01

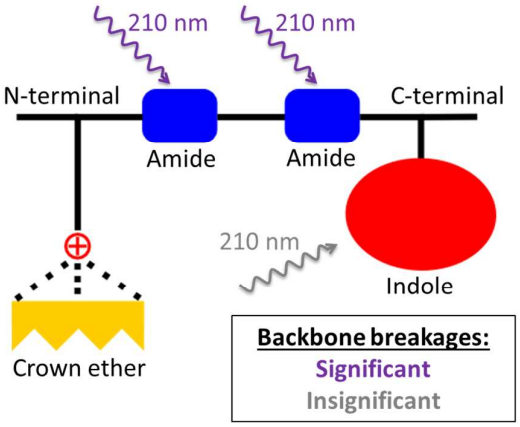

.

To significantly induce backbone dissociation in a prompt process by ultraviolet light, the photon should be absorbed by the amide.